BIOCHEMISTRY
including biophysical chemistry & molecular biology

Article

pubs.acs.org/biochemistry

The N-Terminal Zinc Finger and Flanking Basic Domains Represent the Minimal Region of the Human Immunodeficiency Virus Type-1 Nucleocapsid Protein for Targeting Chaperone Function

Mithun Mitra,[†,∥] Wei Wang,[†] My-Nuong Vo,[‡,⊥] Ioulia Rouzina,[§] George Barany,[‡] and Karin Musier-Forsyth*[,†]

[†]Department of Chemistry and Biochemistry, Center for RNA Biology, and Center for Retrovirus Research, The Ohio State University, Columbus, Ohio 43210, United States

[‡]Department of Chemistry and [§]Department of Biochemistry, Molecular Biology and Biophysics, University of Minnesota, Minneapolis, Minnesota 55455, United States

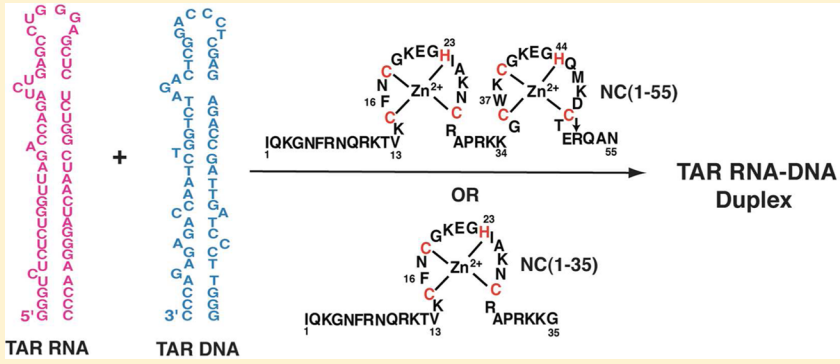

ABSTRACT: The human immunodeficiency virus type-1 (HIV-1) nucleocapsid (NC) protein is a chaperone that facilitates nucleic acid conformational changes to produce the most thermodynamically stable arrangement. The critical role of NC in many steps of the viral life cycle makes it an attractive therapeutic target. The chaperone activity of NC depends on its nucleic acid aggregating ability, duplex destabilizing activity, and rapid on−off binding kinetics. During the minus-strand transfer step of reverse transcription, NC chaperones the annealing of highly structured transactivation response region (TAR) RNA to the complementary TAR DNA. In this work, the role of different functional domains of NC in facilitating 59-nucleotide TAR RNA−DNA annealing was probed by using chemically synthesized peptides derived from full-length (55 amino acids) HIV-1 NC: NC(1−14), NC(15−35), NC(1−28), NC(1−35), NC(29−55), NC(36−55), and NC(11−55). Most of these peptides displayed significantly reduced annealing kinetics, even when present at concentrations much higher than that of wild-type (WT) NC. In addition, these truncated NC constructs generally bind more weakly to single-stranded DNA and are less effective nucleic acid aggregating agents than full-length NC, consistent with the loss of both electrostatic and hydrophobic contacts. However, NC(1−35) displayed annealing kinetics, nucleic acid binding, and aggregation activity that were very similar to those of WT NC. Thus, we conclude that the N-terminal zinc finger, flanked by the N-terminus and linker domains, represents the minimal sequence that is necessary and sufficient for chaperone function *in vitro*. In addition, covalent continuity of the 35 N-terminal amino acids of NC is critical for full activity. Thus, although the hydrophobic pocket formed by residues proximal to the C-terminal zinc finger has been a major focus of recent anti-NC therapeutic strategies, NC(1−35) represents an alternative target for therapeutics aimed at disrupting NC's chaperone function.

HIV-1 nucleocapsid protein (NC) is a 55-amino acid highly basic protein generated as a result of proteolytic cleavage of the gag precursor protein during viral maturation.[1−6] HIV-1 NC has been shown to play roles in different steps of the viral life cycle, including specific viral RNA packaging,[7,8] virus assembly,[9] reverse transcription of viral RNA,[10−12] and proviral DNA integration.[13,14] NC consists of two well-conserved CCHC-type zinc finger motifs that are separated by a short basic linker. The aromatic residues present in the zinc finger motifs stack with nucleobases present in single-stranded (ss) regions of nucleic acids.[15−18] NC also possesses a 14-amino acid flexible N-terminal domain, which has a high local density of basic residues (5 of 14). This N-terminal domain forms a 3_{10}-helix when NC binds to stem loops 2 and 3 of the viral packaging signal.[15,17] NC's numerous roles in the viral life cycle depend, in part, on its nucleic acid chaperone activity, which facilitates nucleic acid rearrangements to form the thermodynamically most stable conformation.[10−12,19] Because of the critical role of

Received: September 9, 2013
Revised: October 18, 2013
Published: October 22, 2013

NC in HIV-1 infection, targeting NC's chaperone function is a viable therapeutic strategy.[20−23]

The nucleic acid chaperone function of NC depends on two main activities: nucleic acid duplex destabilization and aggregation, which are associated with the zinc finger and basic N-terminal domain, respectively.[11,12] In addition, rapid nucleic acid binding kinetics has also been shown to be a critical component of NC's chaperone activity.[24,25] Previous studies have suggested that NC's duplex destabilization activity is more important for reactions in which the rate-limiting step involves significant melting of nucleic acid structure.[12] For example, the zinc finger motifs were shown to be important for annealing of the highly structured transactivation response region (TAR) RNA and TAR DNA stem loops[26] and also for RNA removal reactions during reverse transcription[26−28] but are not needed for annealing of human $tRNA^{Lys3}$ to the primer binding site (PBS) in the viral RNA genome.[29,30] The role of zinc fingers was tested by employing a SSHS NC mutant in which all the Cys residues of the two zinc fingers were mutated to Ser, which abolished its ability to bind zinc.[26] The relative contributions of the N-terminal and C-terminal zinc finger motifs in the chaperone function of NC have also been studied, and the N-terminal zinc finger has been found to play a major role in destabilizing structured nucleic acids.[31−33]

In addition to the destabilization activity of NC's zinc fingers, NC's ability to aggregate nucleic acids facilitates the nucleation step of the annealing reaction.[34−38] This nonspecific nucleic acid aggregation activity of NC is a major component of its chaperone function and contributes to annealing of both structured and nonstructured nucleic acids.[11] While the zinc fingers of NC have also been shown to play a role in aggregating nucleic acids by contributing to NC's binding strength,[36,37] the N-terminal domain of NC is most critical for this activity.[11,34,35]

In addition to the documented roles of the N-terminal domain and zinc fingers in the chaperone activity of NC, the function of synthetic peptides derived from different domains of NC has been investigated in a variety of assays.[39−51] For example, Surovoy et al. performed *in vitro* binding studies using chemically synthesized peptides NC(1−19), NC(36−55), and NC(20−55) and an RNA construct representing the 5′ end of the HIV-1 genome.[44] Both NC(1−19) and NC(20−55) bound to RNA, albeit with affinities 50−200-fold lower than that of WT, while NC(36−55) displayed almost no RNA binding. In a related study, the importance of the N-terminal zinc finger of NC and the flanking basic residues [i.e., NC(1−35)] in promoting specific binding to the ψ-packaging sequence was elucidated.[45]

Peptides representing the proximal (residues 13−30) and distal zinc finger (residues 34−51) motifs were found to be inactive in *in vitro* assays of HIV-1 RNA dimerization, as well as in annealing of primer $tRNA^{Lys3}$ to the PBS.[39] Rocquigny et al. demonstrated the importance of the basic residues flanking the proximal zinc finger of NC in $tRNA^{Lys3}$/PBS annealing and RNA binding.[41] Complete deletion of the zinc fingers did not have any effect on the tRNA annealing activity of NC, and it was concluded that inhibition of the basic residues flanking the first zinc finger of NC could be a model for the design of antiviral agents. This study is consistent with a later study showing that zinc binding was not required for tRNA annealing.[29,30] However, the role of different domains of NC in annealing structured nucleic acids (e.g., TAR RNA−DNA annealing), where zinc fingers play a vital role,[26] was not investigated. In addition, the removal of zinc fingers involved complete deletion of all the amino acids forming the fingers instead of simply removing zinc, thereby maintaining the primary sequence of NC.

In this work, NC fragments representing different domains of NC (Figure 1) were chemically synthesized and their ability to

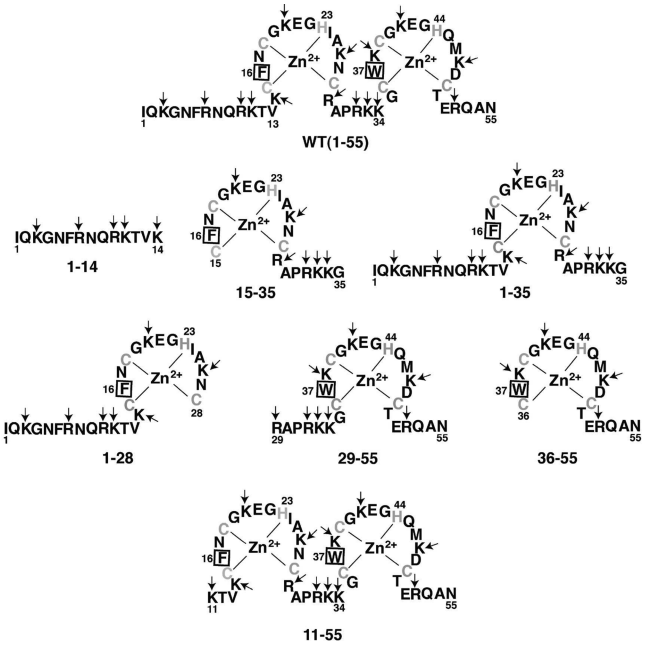

Figure 1. Sequences of chemically synthesized HIV-1 NC (NL4-3 isolate) constructs used in this work: WT NC(1−55), NC(1−14), NC(15−35), NC(1−35), NC(1−28), NC(29−55), NC(36−55), and NC(11−55). The basic residues are denoted with arrows. The aromatic residues in the zinc fingers are boxed. The zinc binding residues are colored gray. Peptides NC(1−35) and NC(29−55) were purchased commercially from Genscript Corp. (Piscataway NJ), whereas all the other peptides were synthesized in house.

chaperone the annealing of 59-nucleotide TAR RNA to complementary 59-nucleotide TAR DNA was tested. As mentioned above, this reaction is known to require the destabilization activity of zinc fingers of NC.[26] Nucleic acid binding and aggregation activity were also evaluated separately to independently gauge their contributions to chaperone activity. The quantitative results reported here indicate that the N-terminal zinc finger flanked with basic N-terminal and linker domains is sufficient to drive the annealing kinetics to an extent similar to that of WT NC and suggest that the C-terminal zinc finger is not important for annealing of structured nucleic acids under the *in vitro* conditions investigated here. Thus, targeting the 35 N-terminal residues of NC is a viable therapeutic strategy aimed at abolishing both specific Gag-ψ RNA binding[45] and NC's chaperone function.

EXPERIMENTAL PROCEDURES

Synthesis of Full-Length and Truncated NC Constructs. The following NC constructs were synthesized using 9-fluorenyl methoxy carbonyl (Fmoc) chemistry: NC(1−55), NC(1−14), NC(1−28), NC(15−35), NC(36−55), and NC(11−55). Solid-phase synthesis was performed on a 433A peptide synthesizer (Applied Biosystems, Foster City, CA) following the general procedure described previously.[51] The crude peptides were purified by reverse-phase high-perform-

dx.doi.org/10.1021/bi401250a | *Biochemistry* 2013, 52, 8226−8236

ance liquid chromatography and analyzed using mass spectrometry. NC(1−35) and NC(29−55) were purchased from Genscript Corp. All lyophilized peptides were reconstituted in 40 mM HEPES (pH 7.5), 5 mM dithiothreitol (DTT), and 0.1 mM tris(2-carboxyethyl)phosphine hydrochloride (TCEP). The reducing agents DTT and TCEP were included in the reconstitution buffer to prevent the formation of disulfide bonds involving the Cys-containing peptides. The concentrations of peptides with a tryptophan residue in the sequence were determined by measuring the absorbance at 280 nm using an extinction coefficient of 6050 M^{-1} cm^{-1}. The concentrations of NC(1−35), NC(1−28), and NC(15−35) were determined by treatment with Ellman's reagent [5,5′-dithiobis(2-nitrobenzoic acid)], which reacts with the sulfhydryl group of accessible Cys residues in a 1:1 ratio and generates a product that can be quantified by measuring the absorbance (extinction coefficient of 14150 M^{-1} cm^{-1} in 0.1 N NaOH) at 412 nm.[52] The concentration of NC(1−14), which is devoid of Trp or Cys residues, was determined using quantitative amino acid analysis (Scientific Research Consortium, Inc., Roseville, MN). Stock solutions of peptides were aliquoted and stored at −80 °C. Poly-L-lysine was purchased from Sigma-Aldrich (St. Louis, MO).

Nucleic Acid Preparation. The sequences and predicted structures (using mfold[53]) of 59-nucleotide TAR RNA and TAR DNA used in this study are shown in Figure 2. The TAR

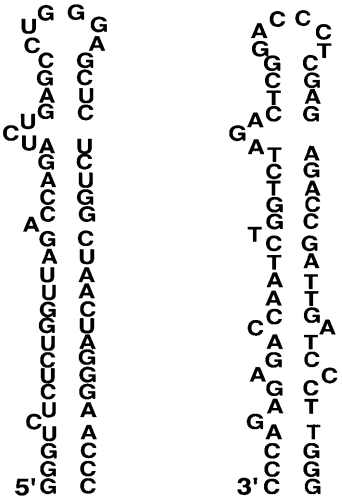

Figure 2. Structures of the 59-nucleotide TAR RNA hairpin (left) and the complementary 59-nucleotide TAR DNA hairpin (right), as predicted by mfold[53] at 37 °C. Sequences are derived from HIV-1 NL4-3.

RNA hairpin was generated by *in vitro* transcription of a DNA template encoding the RNA sequence under the control of a T7 RNA polymerase promoter. This DNA template was prepared by polymerase chain reaction amplification of chemically synthesized oligonucleotides purchased from Integrated DNA Technologies (Coralville, IA). Following transcription, TAR RNA was purified on a 12% denaturing polyacrylamide gel, and its concentration was determined using an extinction coefficient of 533700 M^{-1} cm^{-1} at 260 nm. Internally ^{32}P-labeled TAR RNA was prepared using the same procedure that is described above, except that [α-^{32}P]GTP was employed in the *in vitro* transcription reaction. TAR DNA was obtained from Integrated DNA Technologies and purified on a 12% polyacrylamide gel. The concentration of TAR DNA was determined using an extinction coefficient of 564800 M^{-1} cm^{-1} at 260 nm. The 20-mer sequence 5′-CTTCTTTGGGAGTGAATTAG-3′ (5′-FAM-DNA20) labeled at the 5′ end with the succinimidyl ester of carboxyfluorescein (FAM) was obtained from Trilink BioTechnologies (San Diego, CA).

Gel-Shift Annealing Assay. Prior to each experiment, TAR RNA (1.5 μM) (spiked with ^{32}P-labeled TAR RNA) and TAR DNA (6 μM each) solutions were refolded in 25 mM HEPES (pH 7.5) and 20 mM NaCl by being heated at 80 °C for 2 min and cooled to 60 °C for 2 min, followed by addition of 100 mM $MgCl_2$ (to a final concentration of 10 mM) and placement on ice. For annealing assays, ^{32}P-labeled TAR RNA (15 nM) and TAR DNA (45 nM) were combined in a solution containing 20 mM HEPES (pH 7.5), 20 mM NaCl, and 5 mM DTT. The final concentration of $MgCl_2$ (from the initial folding step) was 0.2 mM. The solution was incubated at 37 °C for 5 min before addition of NC to a final concentration of 0.88 μM, corresponding to a 4:1 nucleotide:NC ratio. Annealing reactions were performed under these standard conditions of nucleic acids, NC, and buffer composition, unless otherwise indicated. At desired time points, an aliquot (27 μL) of the reaction mixture was quenched by addition of 3 μL of 10% SDS (final concentration of 1%), followed by incubation at room temperature (RT) for 5 min and placement on ice. The aliquots were extracted twice with phenol and chloroform (to remove any NC bound to the nucleic acids) followed by addition of glycerol (5%) and separation on a 12% polyacrylamide gel (19% acrylamide:bisacrylamide). The gels were visualized using a Typhoon Trio phosphorimager (GE Healthcare) and quantified with Imagequant TL (version 2005). Rate constants were calculated by fitting the data to a single-exponential equation.

Sedimentation Assay. Both ^{32}P-labeled TAR RNA and TAR DNA were folded as described for annealing assays. The sedimentation assays for measuring aggregation were performed as described previously,[38] by incubating ^{32}P-labeled TAR RNA and TAR DNA at final concentrations of 15 and 45 nM, respectively, in a buffer containing 20 mM HEPES (pH 7.5) and 20 mM NaCl in the absence or presence of different concentrations of NC. The final $MgCl_2$ concentration was 0.2 mM, unless otherwise indicated. The samples (30 μL) were incubated at 37 °C for 30 min and then centrifuged in a Micromax RF rotor at a speed of 10000 rpm for 10 min. An aliquot (4 μL) of supernatant was taken and the amount of radioactivity measured using scintillation counting.

Fluorescence Anisotropy (FA)-Based Binding Assay. The binding of protein to 5′-FAM-DNA20 was measured by incubating 20 nM DNA in the presence of varying concentrations of peptide in 20 mM HEPES (pH 7.5), 50 mM NaCl, 10 μM TCEP, 5 mM β-mercaptoethanol, and 1 μM zinc acetate for 30 min at 25 °C. FA measurements were performed in Corning (Corning, NY) 384-well low-volume polystyrene NBS microplates using a SpectraMax M5 multimode microplate reader (Molecular Devices, Sunnyvale, CA). Excitation and emission wavelengths were set to 485 nm (9 nm bandwidth) and 525 nm (15 nm bandwidth), respectively. Anisotropy was calculated using SoftMax Pro (Molecular Devices). The resulting plot of anisotropy versus NC concentration was fit using Kaleidagraph (Synergy Software, Reading, PA) according to the following one-site binding model[54] to obtain apparent dissociation constant (K_d):

$$A = \frac{A_{free} + (\{T + N + K_d - [(T + N + K_d)^2 - (4TN)]^{1/2}\}/2T)(RA_{bound} - A_{free})}{(R - 1)(\{T + N + K_d - [(T + N + K_d)^2 - (4TN)]^{1/2}\}/2T) + 1}$$

where T, N, K_d, A_{bound}, A_{free}, and R represent the concentrations of oligonucleotide and protein, the equilibrium dissociation constant, the anisotropy of completely bound and unbound oligonucleotide, and the ratio of fluorescence intensity of completely bound oligonucleotide relative to that of unbound nucleotide, respectively. For binding assays performed using zinc-less NC constructs and NC(1−14), zinc acetate was omitted from the reaction buffer.

RESULTS

NC preferentially binds to ss nucleic acids, and this binding preference is crucial for its chaperone function, which involves nucleic acid aggregation and duplex destabilization activities. Binding capability general correlates closely with aggregation activity, which is facilitated mainly by NC's basic residues. In contrast, the zinc finger structures are primarily responsible for nucleic acid destabilization capability, which is essential for annealing of stable stem−loop substrates such as the TAR RNA−DNA forms investigated here. Chemically synthesized full-length HIV-1 NC (55 amino acids) and NC fragments (Figure 1) were used to explore in more detail the specific roles of different domains of NC in mediating nucleic acid binding, aggregation, and complementary TAR RNA−DNA annealing. The theoretical isoelectric point (pI) of all the NC constructs was calculated using the Protparam web-based program,[55] and these values are listed in Table 1. Unless otherwise noted, all of the NC constructs containing CCHC motif(s) were reconstituted with 3 equiv of zinc prior to the assays.

Nucleic Acid Binding. The results of fluorescence anisotropy (FA) binding studies conducted with the NC fragments and 5′-FAM-DNA20 are summarized in Table 1. A nonspecific ss DNA was chosen for these studies to avoid any complications caused by RNA folding or NC's duplex destabilization activity. WT NC binds to this DNA with a dissociation constant (K_d) of 57 nM, and NC(1−35) demonstrated a similar binding affinity, with a K_d of 86 nM. NC(15−35) bound with an at least ∼116-fold lower affinity than NC(1−35), confirming an important role in nucleic acid binding for the electrostatic interactions provided by the highly basic N-terminal domain. Removal of the linker domain from NC(1−35) to generate NC(1−28) led to an ∼8.5-fold reduction in binding affinity. Thus, at 50 mM NaCl, the N-terminal and linker domains flanking the proximal zinc finger provide the major contribution to binding. The results for NC(15−35) and NC(1−28) also reveal the greater contribution of the N-terminal domain to binding relative to that of the linker region. Surprisingly, no binding could be detected by the highly basic NC(1−14) domain alone.

NC(29−55) has an ∼15-fold lower ss DNA binding affinity than WT NC, with a K_d of 867 nM. Although NC(15−35) and NC(29−55) both include the basic linker domain and have similar pI values, the binding affinity of NC(15−35) was measured to be at least ∼12-fold weaker than that of NC(29−55). The hydrophobic pockets formed by the residues of the zinc fingers of NC have been shown to interact specifically with unpaired guanosine residues of single-stranded sequences,[8,12,18] and the aromatic residues Phe16 and Trp37 stack with the guanosine bases. The results reported here are consistent with the previously observed stacking interactions of Trp37 [present in NC(29−55)] that are stronger than those of Phe16 [present in NC(15−35)].[56,57]

The effect of zinc coordination to the CCHC motif(s) present in WT NC, NC(1−35), NC(1−28), and NC(29−55) was probed by performing binding studies in the absence of zinc (i.e., the synthetic peptides were not reconstituted with zinc, and the reaction buffer did not contain Zn^{2+}). In the case of WT NC, the zinc-bound protein has a slightly lower affinity (∼4-fold) than the zinc-less form (Table 1), suggesting that the zinc finger structure is not critical for nucleic acid binding under the low-salt conditions employed here, where nonspecific electrostatic interactions likely dominate. Interestingly, zinc coordination has the opposite effect on binding by NC(1−35), NC(1−28), and NC(29−55) sequences; the zinc-bound forms have slightly higher affinities (∼2−3-fold) for 5′-FAM-DNA20 than the zinc-less variants (Table 1). This is likely due to the enhanced role of the folded zinc fingers for these peptides, which lack the additional electrostatic interactions conferred by the basic residues in the deleted regions.

Nucleic Acid Aggregation. NC has been shown to form ordered aggregates with nucleic acids,[37,38,58−61] and this activity facilitates nucleation of the product duplex during annealing reactions. Saturated NC binding is required for maximal aggregation activity, and the NC concentration dependence of fractional nucleic acid aggregation reflects the protein's binding strength.[38] To monitor the contribution of different domains of NC in nucleic acid aggregation, sedimentation assays were performed using varying concentrations of WT NC and NC fragments under conditions similar to those used for TAR RNA−DNA annealing assays (see Experimental Procedures and results described below). All of the NC constructs containing CCHC motif(s) were reconstituted with 3 equiv of zinc, unless noted otherwise. Results of sedimentation assays

Table 1. Theoretical Isoelectric Points (pI) of WT NC and NC Fragments and Their Apparent Binding Dissociation Constants (K_d) with 5′-FAM-DNA20

	pI[a]	K_d[b] (nM)
WT	9.93	57 ± 22
WT (zinc-less)	9.93	16 ± 5
NC(1−14)	12.02	≥1 × 10^4
NC(15−35)	9.75	≥1 × 10^4
NC(1−35)	10.71	86 ± 19
NC(1−35) (zinc-less)	10.71	296 ± 170
NC(1−28)	9.93	731 ± 150
NC(1−28) (zinc-less)	9.93	1600 ± 309
NC(29−55)	9.65	867 ± 3
NC(29−55) (zinc-less)	9.65	1835 ± 370
NC(36−55)	7.95	not determined
NC(11−55)	9.54	not determined

[a]pI values were computed using the ProtParam program.[55] [b]FA binding experiments were performed in 20 mM HEPES (pH 7.5), 50 mM NaCl, 5 mM β-mercaptoethanol, 10 μM TCEP, and 1 μM zinc acetate at 25 °C. For binding studies using the zinc-less NC constructs or NC(1−14), no zinc acetate was present. Values reported represent the average of three trials with the standard deviation indicated.

dx.doi.org/10.1021/bi401250a | Biochemistry 2013, 52, 8226−8236

are depicted in Figure 3. WT NC displayed very high levels (~97%) of nucleic acid aggregation, even at a concentration of

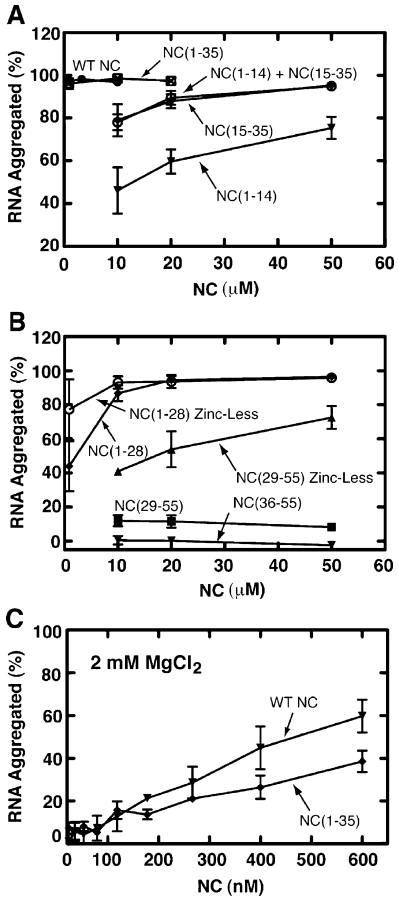

Figure 3. RNA aggregation assays for WT NC and truncated NC peptides. (A) Assays performed with 0.88–20 μM WT NC and NC(1–35) and 10–50 μM NC(1–14) and NC(15–35) alone or added together *in trans*. (B) Assays with 0.88–50 μM NC(1–28) in the presence and absence of zinc, 10–50 μM NC(29–55) in the presence and absence of zinc, and 10–50 μM NC(36–55). (C) Assays performed with 23–600 nM WT NC and NC(1–35) in the presence of 2 mM $MgCl_2$.

0.88 μM. As expected, aggregation levels did not change appreciably with increases in the concentration of WT NC to 3 and 10 μM. Similar to WT NC, NC(1–35) aggregated ~96% of the nucleic acids, even at 0.88 μM peptide (Figure 3A). This result suggests that the distal zinc finger is not important for nucleic acid aggregation. Under these relatively low salt conditions, close to 100% aggregation was observed for WT NC and NC(1–35) at the lowest concentration tested (0.88 μM), precluding comparison of their relative activities. Therefore, we also studied aggregation activities of these proteins at much lower protein concentrations and in the presence of 2 mM $MgCl_2$. Mg^{2+} competes effectively with low concentrations of both WT NC and NC(1–35), making it possible to observe any differences in binding and aggregation ability, which appear to be minor (Figure 3C).

NC(1–14) and NC(15–35) demonstrated concentration-dependent aggregation behavior over the peptide concentration range of 10–50 μM with lower levels observed for NC(1–14) (Figure 3A). Previous studies showed that deletion of part of the N-terminal domain from the WT sequence resulted in almost total abrogation of the nucleic acid aggregating ability of NC.[34,35] However, the aggregation behavior of the isolated N-terminal domain was not addressed previously. Results presented here for NC(1–14) suggest that the N-terminal domain by itself is not sufficient for efficient nucleic acid aggregation. When present at a high concentration (50 μM), NC(15–35) showed almost WT levels (~95%) of aggregation, whereas NC(1–14) achieved only ~80% of the WT level. When NC(1–14) and NC(15–35) are present in *trans*, their ability to induce nucleic acid aggregation does not exceed that of NC(15–35) (Figure 3A). Thus, covalent continuity of NC(1–14) and NC(15–35) is required for efficient aggregation activity.

NC(1–28) showed ~2.2-fold lower aggregation levels than NC(1–35) at 0.88 μM, suggesting a role for the basic linker domain in aggregation activity (Figure 3A,B). The aggregation activity of NC(1–28) approached that of NC(1–35) at concentrations of ≥20 μM, in good agreement with the annealing activity results (see below). NC(36–55) and NC(29–55) displayed extremely poor aggregation capability and showed no appreciable change in aggregation levels when their concentrations were increased from 10 to 50 μM (Figure 3B); the levels of aggregation at 50 μM remained at ~0 and ~8% for NC(36–55) and NC(29–55), respectively. The slightly higher level of aggregation for NC(29–55) is likely conferred by the additional basic linker domain, which may enhance nonspecific electrostatic interactions with nucleic acids.

Previous studies have shown that the aggregation ability of WT NC does not strongly depend on its folded zinc fingers.[29,30,34] To assess if this holds true for NC fragments as well, we performed sedimentation assays using NC(1–28), NC(1–35), and NC(29–55) in the absence of zinc, at the same concentrations employed for the zinc-bound forms. In the case of NC(1–35), no appreciable differences in aggregation levels were observed in the presence or absence of zinc, and essentially complete aggregation was observed in both cases (data not shown). In the case of NC(29–55), zinc does appear to modulate nucleic acid aggregation behavior, because the levels of aggregation observed for the zinc-less form are higher than those of the zinc-bound form by ~4–7-fold at all concentrations tested (Figure 3B). In addition, and in contrast to the zinc-bound form, the zinc-less form of NC(29–55) showed concentration-dependent aggregation behavior, with aggregation levels increasing from 40 to 72% with an increase in the peptide concentration from 10 to 50 μM, respectively. NC(1–28) showed ~1.7-fold lower aggregation activity than its zinc-less form at the lowest concentration tested (0.88 μM), but both forms showed similar activities at high concentrations. Taken together, these results suggest that the absence of zinc may enhance the aggregation behavior of some NC-derived peptides by transforming their rigid zinc-bound structures to more mobile peptides. In addition, the C-terminal zinc finger is modulated more strongly by zinc binding than the N-terminal zinc finger, in agreement with the more hydrophobic and less cationic character of the C-terminal domain nucleic acid binding interaction.

TAR RNA–DNA Annealing. The overall chaperone function of WT NC and truncated NC fragments was determined by performing time course annealing assays to measure the ability of the peptides to anneal complementary TAR RNA and TAR DNA hairpins (Figure 2) to form a 59 bp duplex. Figure 4 shows the percent of TAR RNA annealed over

dx.doi.org/10.1021/bi401250a | *Biochemistry* 2013, 52, 8226–8236

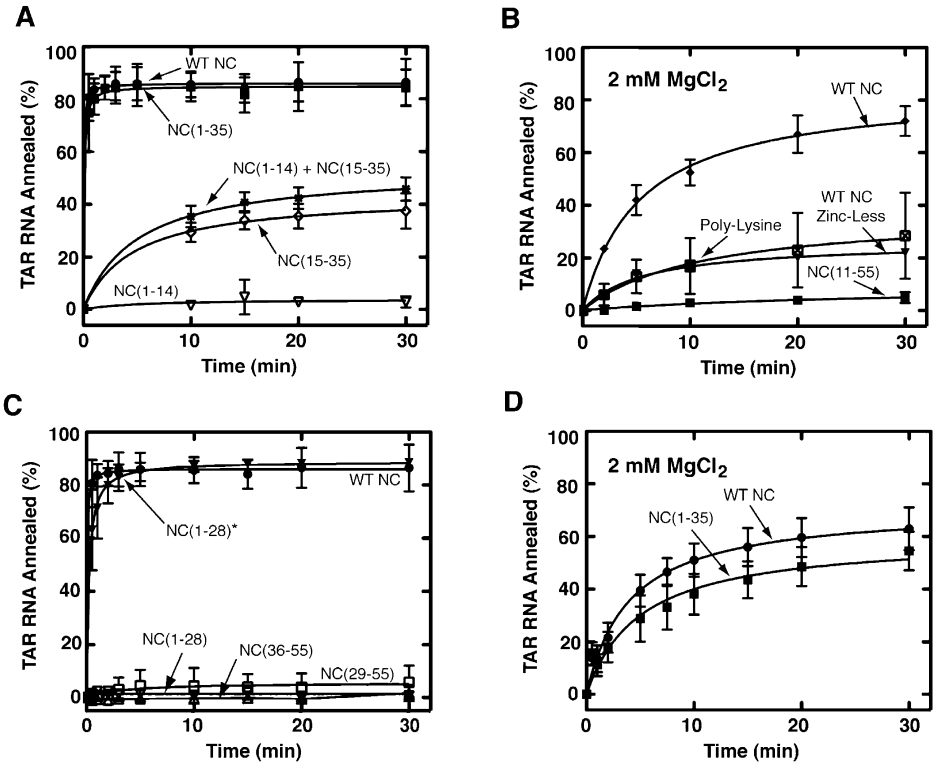

Figure 4. TAR RNA−DNA annealing time courses for WT NC and truncated NC peptides. (A) Reactions with WT NC and NC(1−35) were performed with 0.88 μM peptide. NC(1−14), NC(15−35), and NC(1−14) with NC(15−35) were all present at 20 μM. (B) Reactions using 4 μM WT NC in the presence and absence of zinc (zinc-less), 3 μM polylysine, and 20 μM NC(11−55) performed in the presence of 90 nM TAR DNA and 2 mM $MgCl_2$. (C) Reactions with WT NC and NC(1−28) were performed with 0.88 μM peptide, 20 μM NC(1−28)*, 50 μM NC(29−55) and 50 μM NC(36−55). (D) Reactions using 0.88 μM WT NC and NC(1−35) performed in the presence of 2 mM $MgCl_2$. Results are the average of three trials with standard deviations indicated.

time, and the annealing rate constants are listed in Table 2. Under saturating binding conditions (0.88 μM and 4:1 nucleotide:NC ratio[11]), WT NC displayed very fast annealing kinetics, with 80% of the RNA annealed within 30 s and 86% annealed product formed at 30 min (Figure 4A). Because of the fast reaction rate observed for WT, we could measure only the lower limit for the annealing rate constant under these conditions (Table 2).

Table 2. Annealing Rate Constants (k_{obs}) of WT NC and NC Variants

	final % annealing	k_{obs} (min^{-1})[a]	x-fold decrease[b]
WT, 0.88 μM	86	>4	−
NC(1−14), 20 μM	3	not determined	
NC(1−35), 0.88 μM	84	>4	−
NC(15−35), 20 μM	37	0.15 ± 0.03	≥600
NC(1−14) and NC(15−35), 20 μM each	46	0.15 ± 0.01	≥600
NC(1−28), 20 μM	88	2.7 ± 1.5	≥33
NC(36−55), 50 μM	1.5	not determined	
NC(29−55), 50 μM	6	not determined	0
WT, 0.88 μM[c]	63	0.22 ± 0.04	−
NC(1−35), 0.88 μM[c]	54	0.17 ± 0.07	1.3
WT, 4 μM[d]	72	0.12 ± 0.01	−
WT (zinc-less), 4 μM[d]	22	0.07 ± 0.02	2
polylysine, 3 μM[d]	28	0.03 ± 0.01	3
NC(11−55), 20 μM[d]	5	0.009 ± 0.002	∼70

[a]Values reported represent the average of three trials with the standard deviation indicated. [b]Values are normalized for differences in protein concentrations used. The x-fold decrease was calculated relative to the rate constant for WT NC obtained under the same conditions. [c]Experiments performed at 2 mM $MgCl_2$. [d]Experiments performed using 90 nM TAR DNA and 2 mM $MgCl_2$.

NC(1−14), which has five basic residues in its sequence, exhibited a very poor ability to anneal the TAR RNA−DNA duplex even at 20 μM (∼20-fold higher than that of WT), with only 3% RNA annealed after 30 min (Figure 4A). The level of annealing after 30 min did not change appreciably even when the concentration of NC(1−14) was increased to 50 μM (data not shown), in agreement with the extremely poor binding observed for this peptide (Table 1). NC(1−14) represents the major aggregation domain of WT NC[11,12] and behaves as a flexible short polycation. To evaluate if longer polycations could better facilitate the annealing reaction, we performed annealing assays using zinc-less WT NC and polylysine (Figure 4B). The latter has been shown to be a highly efficient nucleic acid aggregating agent.[62] The results showed that these longer unstructured polycations have 2−3-fold reduced annealing activity compared to that of WT NC (Figure 4B and Table 2). These results support a role for the zinc fingers in destabilizing the TAR stem−loop structures during the annealing reaction.[12]

The annealing activity of NC(36−55), even at 50 μM, is also very poor, with final levels of annealing after 30 min reaching only ∼1.5% (Figure 4C), consistent with this variant's low net positive charge density (pI = 7.9) due to four basic and three acidic residues. Addition of the highly basic linker domain to NC(36−55), thus generating NC(29−55), did not significantly improve the annealing activity. The final levels of RNA

dx.doi.org/10.1021/bi401250a | Biochemistry 2013, 52, 8226−8236

annealed after 30 min for NC(29−55) approached 6% (Figure 4C). Results obtained for NC(36−55) and NC(29−55) suggest that the distal zinc finger may not be important for annealing of the TAR RNA−DNA duplex under the low-salt conditions used here.

In contrast, at 20 μM, NC(15−35) displayed significant annealing activity, despite the fact that it lacked the C-terminal zinc finger; ∼38% RNA−DNA duplex was formed after 30 min (Figure 4A). Previous studies suggested that the N-terminal zinc finger is more important for destabilizing structured nucleic acids than the C-terminal zinc finger,[31,33] in accord with the results obtained here.

Even in the presence of 20 μM NC(15−35), the rate of annealing of this variant is significantly reduced (>600-fold) relative to that of WT NC (Table 2), which suggests that the presence of the proximal zinc finger connected to the basic linker contributes to the annealing but is not sufficient for optimal chaperone activity. In contrast, NC(1−35), which consists of the proximal zinc finger flanked by the basic N-terminal and linker domains, displays annealing kinetics at or close to the lower limit established for WT NC at the same concentration (0.88 μM), with ∼75% of RNA annealed within 30 s (Figure 4A and Table 2). To better differentiate the annealing activities of NC(1−35) and WT NC, annealing assays were conducted at a higher Mg^{2+} concentration (2 mM $MgCl_2$), conditions at which the kinetics of annealing are known to be reduced.[60,63] While TAR binding by WT NC and NC(1−35) is likely saturating under these conditions, Mg^{2+} is known to stabilize the TAR RNA and DNA hairpins, thereby slowing the annealing reaction. Even under these conditions, NC(1−35) showed annealing activity similar to that of WT NC (Figure 4D). The final levels of annealing were ∼63 and ∼55% for WT and NC(1−35), respectively, and the annealing rate constant for NC(1−35) was only ∼1.3-fold lower than that of WT (Table 2). Thus, as for the binding and aggregation assays, NC(1−35) represents the minimal region, containing the necessary sequence and structural elements required for efficient TAR RNA−DNA annealing.

To determine the effect of adding NC(1−14) and NC(15−35) together, both peptides were used at equal concentrations of 20 μM in the annealing reaction (Figure 4A). The activity of the two domains *in trans* was much lower than the activity of NC(1−35) at 0.88 μM. The final level of annealing and the k_{obs} were very similar to that of NC(15−35) (Table 2). This suggests that as for aggregation activity, covalent continuity of NC(1−35) is essential for optimal chaperone function. Consistent with this observation, NC lacking the 10 N-terminal amino acid residues, NC(11−55), is highly deficient in annealing the TAR RNA−DNA duplex, even at a protein concentration 5-fold higher than that of WT NC (Figure 4B). These observations indicate that the N-terminal region of NC plays an important role in NC's annealing activity presumably by promoting nucleic acid aggregation. Comparison of the two peptides containing the first or second zinc finger in combination with the cationic linker, i.e., NC(15−35) and NC(29−55), in their TAR RNA−DNA annealing (Figure 4A,C) highlights the much stronger activity of the first zinc finger, in agreement with its stronger TAR RNA−DNA binding under the same solution conditions (Figure 3A,B).

To probe the role of the linker domain in the activity of NC(1−35), we performed annealing assays using NC(1−28), which lacks the basic linker region. This variant demonstrated very poor annealing activity at 0.88 μM, suggesting an important role for the linker domain in the chaperone activity of NC(1−35) (Figure 4C). However, 20 μM NC(1−28) showed activity almost equal to that of 0.88 μM NC(1−35) (Figure 4A,C). Under these conditions, the extents of annealing at the shortest time point tested (30 s) were ∼63 and ∼75% for NC(1−28) and NC(1−35), respectively. This result suggests that the basic residues of the linker domain (R29, R32, K33, and K34) contribute to nucleic acid binding and not to destabilization activity by increasing the overall positive charge of NC(1−35).

DISCUSSION

This study using NC fragments was performed to delineate the roles played by different domains of NC in its nucleic acid chaperone function. Targeting this critical function of NC is a promising therapeutic strategy. Studies of TAR RNA−DNA annealing, nucleic acid aggregation, and ss DNA binding suggest that the C-terminal domain of NC (i.e., residues 36−55) is not required for NC's chaperone function. The presence of the N-terminal zinc finger flanked by the highly basic N-terminus and linker domains is sufficient to achieve binding, aggregation, and annealing activities similar to those of WT NC. Previous studies have shown that folded zinc fingers are important for TAR RNA−DNA annealing[26] and that the N-terminal zinc finger is especially crucial for annealing structured substrates.[31,33] The similar nucleic acid chaperone abilities of WT NC and NC(1−35) suggest that the C-terminal zinc finger is dispensable for annealing structured nucleic acids such as the TAR RNA−DNA duplex.

Because complete nucleic acid aggregation was observed by WT NC or by NC(1−35), with and without bound zinc, it appears that zinc coordination is not required for aggregation activity. Indeed, polycations with little, if any, apparent structure have been shown to be effective nucleic acid aggregating agents,[11,64,65] which correlates with the results presented here. Furthermore, the zinc-less variants of NC(29−55) and NC(1−28) are more efficient in aggregating nucleic acids than the zinc-bound forms, which may be due to the presence of greater flexibility in the peptide backbone of the zinc-less forms. Our conclusion that the folded zinc finger structures of NC are not required for effective nucleic acid aggregation is not in agreement with previous electron microscopy studies.[37] The previous work employed higher Mg^{2+} concentrations, as well as much longer nucleic acid sequences, which may result in a different mechanism of NC-induced nucleic acid aggregation.

Another interesting finding from our work was that the isolated NC(1−14) peptide is less effective in promoting nucleic acid aggregation, binding, or annealing than WT NC or NC(1−35), despite the fact that this is the main "aggregation domain" in the context of full-length NC.[11,12] Indeed, annealing studies with NC(11−55) support the key role played by the N-terminal residues in chaperone function. Adding NC(1−14) to NC(15−35) *in trans* also failed to improve activities of the isolated domains. Thus, the N-terminal domain of NC cannot function as an independent chaperone protein but can strongly enhance the chaperone function of NC when covalently connected to the zinc fingers.

The nucleic acid binding affinity of NC is closely coupled to its nucleic acid aggregating activity.[11] Results of binding measurements using a ss DNA oligonucleotide indicate that, with the exception of NC(1−35), which has a K_d within 2-fold of that of WT NC, truncated constructs have significantly lower

affinity (>10-fold) than the full-length sequence. Although an unstructured ss DNA oligonucleotide was used in this work, the binding affinities of different NC constructs could still be compared, given that nucleic acid chaperones generally do not recognize a specific sequence. Previous studies that examined binding to the ψ-RNA packaging signal also concluded that specific binding by HIV-1 NC requires NC(1−35).[45]

Whereas WT NC displays somewhat stronger binding in the absence of zinc, enhanced binding is observed for zinc-bound forms of the truncated constructs tested. These binding results for NC fragments [except NC(1−35)] are in contrast to their aggregation abilities, where zinc-less forms are generally better in aggregating nucleic acids than zinc-bound forms. With fewer basic residues in NC fragments, the presence of at least one folded zinc finger domain enhances binding to ss DNA, whereas unstructured fragments are more capable of aggregating nucleic acids than their structured counterparts. NC(15−35) has appreciable TAR RNA−DNA annealing and aggregation activities, even though it binds to ss DNA very poorly. This is in agreement with the conclusion that the N-terminal zinc finger is important for chaperone activity.

NC has been proposed to be an effective therapeutic target because of its important role in HIV-1 replication.[12,20−23] NC possesses two invariant CCHC zinc fingers, and several studies have focused on the development of small molecule inhibitors that function by ejecting zinc and thus inhibiting NC's activity.[23,66,67] The challenge here is to generate compounds that specifically interact with NC, without inadvertently affecting the zinc fingers associated with cellular proteins such as transcription factors. Inhibitors that function by binding to the NC protein without chelating zinc may therefore represent a more promising strategy. Recently, efforts to target different aspects of NC function such as nucleic acid binding, annealing, and duplex destabilization activities have been reported.[68−79] Several of these inhibitors function via binding to the hydrophobic pocket of NC formed by the zinc finger motifs.[72,74,76,77,79]

This study has identified the first 35 residues of NC as being sufficient for its chaperone function. Because this is also the minimal domain for conferring specific ψ-RNA binding,[45] small molecule inhibitors targeting this minimal domain could potentially block two important NC activities, i.e., genomic RNA packaging and nucleic acid chaperone function. Alternatively, this minimal construct, with its specific cationic and hydrophobic features, could be used as a starting point to synthesize peptidomimetic compounds with enhanced binding affinities for NC substrates. Although our results show that the C-terminal zinc finger is not essential for NC's chaperone activity *in vitro*, the numerous functions of NC *in vivo* likely involve important contributions of both zinc fingers. Nevertheless, the identification of the minimal domain required for chaperone function might provide a platform for the development of a new class of NC-targeted therapeutics.

AUTHOR INFORMATION

Corresponding Author

*Address: 100 W. 18th Ave., Department of Chemistry and Biochemistry, The Ohio State University, Columbus, OH 43210. E-mail: musier@chemistry.ohio-state.edu. Telephone: (614) 292-2021.

Present Addresses

[‖]Section on Viral Gene Regulation, Program in Genomics of Differentiation, Eunice Kennedy Shriver National Institute of Child Health and Human Development, National Institutes of Health, Bethesda, MD 20892−2780.

[⊥]Skaggs Institute for Chemical Biology and Department of Cell and Molecular Biology, The Scripps Research Institute, La Jolla, CA 92037.

Funding

This work was supported by National Institutes of Health Grant GM065056 to K.M.-F.

Notes

The authors declare no competing financial interest.

ACKNOWLEDGMENTS

We thank Drs. Brandie Kovaleski and Daniel G. Mullen for help in the chemical synthesis of WT NC protein and Dr. Daniel G. Mullen for the synthesis of NC(1−14), NC(1−28), NC(15−35), and NC(36−55) peptides. We also thank Drs. Kristen Stewart-Maynard and Christopher P. Jones for helpful and stimulating discussions.

ABBREVIATIONS

NC, nucleocapsid; HIV-1, human immunodeficiency virus type-1; TAR, transactivation response region; PBS, primer-binding site; Fmoc, 9-fluorenyl methoxy carbonyl; DTT, dithiothreitol; TCEP, tris(2-carboxyethyl)phosphine hydrochloride; FAM, carboxyfluorescein; ss, single-stranded; K_d, dissociation constant.

REFERENCES

(1) Mervis, R. J., Ahmad, N., Lillehoj, E. P., Raum, M. G., Salazar, F. H. R., Chan, H. W., and Venkatesan, S. (1988) The *gag* gene products of human immunodeficiency virus type 1: Alignment within the *gag* open reading frame, identification of posttranslational modifications, and evidence for alternative *gag* precursors. *J. Virol. 62*, 3993−4002.

(2) Henderson, L. E., Bowers, M. A., Sowder, R. C., II, Serabyn, S. A., Johnson, D. G., Bess, J. W., Jr., Arthur, L. O., Bryant, D. K., and Fenselau, C. (1992) Gag proteins of the highly replicative MN strain of human immunodeficiency virus type 1: Posttranslational modifications, proteolytic processings, and complete amino acid sequences. *J. Virol. 66*, 1856−1865.

(3) Wondrak, E. M., Louis, J. M., de Rocquigny, H., Chermann, J. C., and Roques, B. P. (1993) The gag precursor contains a specific HIV-1 protease cleavage site between the NC (P7) and P1 proteins. *FEBS Lett. 333*, 21−24.

(4) Coffin, J. M., Hughes, S. H., and Varmus, H. E. (1997) *Retroviruses*, Cold Spring Harbor Laboratory Press, Plainview, NY.

(5) Briggs, J. A. G., and Kräusslich, H.-G. (2011) The molecular architecture of HIV. *J. Mol. Biol. 410*, 491−500.

(6) Lee, S.-K., Potempa, M., and Swanstrom, R. (2012) The choreography of HIV-1 proteolytic processing and virion assembly. *J. Biol. Chem. 287*, 40867−40874.

(7) Gorelick, R. J., Nigida, S. M., Jr., Bess, J. W., Jr., Arthur, L. O., Henderson, L. E., and Rein, A. (1990) Noninfectious human immunodeficiency virus type 1 mutants deficient in genomic RNA. *J. Virol. 64*, 3207−3211.

(8) Lu, K., Heng, X., and Summers, M. F. (2011) Structural determinants and mechanism of HIV-1 genome packaging. *J. Mol. Biol. 410*, 609−633.

(9) Muriaux, D., and Darlix, J.-L. (2010) Properties and functions of the nucleocapsid protein in virus assembly. *RNA Biol. 7*, 744−753.

(10) Bampi, C., Jacquenet, S., Lener, D., Décimo, D., and Darlix, J.-L. (2004) The chaperoning and assistance roles of the HIV-1 nucleocapsid protein in proviral DNA synthesis and maintenance. *Int. J. Biochem. Cell Biol. 36*, 1668−1686.

(11) Levin, J. G., Guo, J., Rouzina, I., and Musier-Forsyth, K. (2005) Nucleic acid chaperone activity of HIV-1 nucleocapsid protein: Critical

role in reverse transcription and molecular mechanism. *Prog. Nucleic Acid Res. Mol. Biol. 80*, 217−286.
(12) Levin, J. G., Mitra, M., Mascarenhas, A., and Musier-Forsyth, K. (2010) Role of HIV-1 nucleocapsid protein in HIV-1 reverse transcription. *RNA Biol. 7*, 754−774.
(13) Thomas, J. A., Gagliardi, T. D., Alvord, W. G., Lubomirski, M., Bosche, W. J., and Gorelick, R. J. (2006) Human immunodeficiency virus type 1 nucleocapsid zinc-finger mutations cause defects in reverse transcription and integration. *Virology 353*, 41−51.
(14) Thomas, J. A., and Gorelick, R. J. (2008) Nucleocapsid protein function in early infection processes. *Virus Res. 134*, 39−63.
(15) De Guzman, R. N., Wu, Z. R., Stalling, C. C., Pappalardo, L., Borer, P. N., and Summers, M. F. (1998) Structure of the HIV-1 nucleocapsid protein bound to the SL3 ψ-RNA recognition element. *Science 279*, 384−388.
(16) Fisher, R. J., Rein, A., Fivash, M., Urbaneja, M. A., Casas-Finet, J. R., Medaglia, M., and Henderson, L. E. (1998) Sequence-specific binding of human immunodeficiency virus type 1 nucleocapsid protein to short oligonucleotides. *J. Virol. 72*, 1902−1909.
(17) Amarasinghe, G. K., De Guzman, R. N., Turner, R. B., Chancellor, K. J., Wu, Z. R., and Summers, M. F. (2000) NMR structure of the HIV-1 nucleocapsid protein bound to stem-loop SL2 of the ψ-RNA packaging signal. Implications for genome recognition. *J. Mol. Biol. 301*, 491−511.
(18) Darlix, J.-L., Godet, J., Ivanyi-Nagy, R., Fossé, P., Mauffret, O., and Mély, Y. (2011) Flexible nature and specific functions of the HIV-1 nucleocapsid protein. *J. Mol. Biol. 410*, 565−581.
(19) Rein, A., Henderson, L. E., and Levin, J. G. (1998) Nucleic-acid-chaperone activity of retroviral nucleocapsid proteins: Significance for viral replication. *Trends Biochem. Sci. 23*, 297−301.
(20) Darlix, J.-L., Cristofari, G., Rau, M., Péchoux, C., Berthoux, L., and Roques, B. (2000) Nucleocapsid protein of human immunodeficiency virus as a model protein with chaperoning functions and as a target for antiviral drugs. *Adv. Pharmacol. 48*, 345−372.
(21) Musah, R. A. (2004) The HIV-1 nucleocapsid zinc finger protein as a target of antiretroviral therapy. *Curr. Top. Med. Chem. 4*, 1605−1622.
(22) de Rocquigny, H., Shvadchak, V., Avilov, S., Dong, C. Z., Dietrich, U., Darlix, J.-L., and Mély, Y. (2008) Targeting the viral nucleocapsid protein in anti-HIV-1 therapy. *Mini Rev. Med. Chem. 8*, 24−35.
(23) Mori, M., Manetti, F., and Botta, M. (2011) Targeting protein-protein and protein-nucleic acid interactions for anti-HIV therapy. *Curr. Pharm. Des. 17*, 3713−3728.
(24) Cruceanu, M., Gorelick, R. J., Musier-Forsyth, K., Rouzina, I., and Williams, M. C. (2006) Rapid kinetics of protein-nucleic acid interaction is a major component of HIV-1 nucleocapsid protein's nucleic acid chaperone function. *J. Mol. Biol. 363*, 867−877.
(25) Wu, H., Rouzina, I., and Williams, M. C. (2010) Single-molecule stretching studies of RNA chaperones. *RNA Biol. 7*, 712−723.
(26) Guo, J., Wu, T., Anderson, J., Kane, B. F., Johnson, D. G., Gorelick, R. J., Henderson, L. E., and Levin, J. G. (2000) Zinc finger structures in the human immunodeficiency virus type 1 nucleocapsid protein facilitate efficient minus- and plus-strand transfer. *J. Virol. 74*, 8980−8988.
(27) Post, K., Kankia, B., Gopalakrishnan, S., Yang, V., Cramer, E., Saladores, P., Gorelick, R. J., Guo, J., Musier-Forsyth, K., and Levin, J. G. (2009) Fidelity of plus-strand priming requires the nucleic acid chaperone activity of HIV-1 nucleocapsid protein. *Nucleic Acids Res. 37*, 1755−1766.
(28) Hergott, C. B., Mitra, M., Guo, J., Wu, T., Miller, J. T., Iwatani, Y., Gorelick, R. J., and Levin, J. G. (2013) Zinc finger function of HIV-1 nucleocapsid protein is required for removal of 5′-terminal genomic RNA fragments: A paradigm for RNA removal reactions in HIV-1 reverse transcription. *Virus Res. 171*, 346−355.
(29) Hargittai, M. R. S., Mangla, A. T., Gorelick, R. J., and Musier-Forsyth, K. (2001) HIV-1 nucleocapsid protein zinc finger structures induce $tRNA^{Lys,3}$ structural changes but are not critical for primer/template annealing. *J. Mol. Biol. 312*, 985−997.
(30) Hargittai, M. R. S., Gorelick, R. J., Rouzina, I., and Musier-Forsyth, K. (2004) Mechanistic insights into the kinetics of HIV-1 nucleocapsid protein-facilitated tRNA annealing to the primer binding site. *J. Mol. Biol. 337*, 951−968.
(31) Heath, M. J., Derebail, S. S., Gorelick, R. J., and DeStefano, J. J. (2003) Differing roles of the N- and C-terminal zinc fingers in human immunodeficiency virus nucleocapsid protein-enhanced nucleic acid annealing. *J. Biol. Chem. 278*, 30755−30763.
(32) Beltz, H., Clauss, C., Piémont, E., Ficheux, D., Gorelick, R. J., Roques, B., Gabus, C., Darlix, J.-L., de Rocquigny, H., and Mély, Y. (2005) Structural determinants of HIV-1 nucleocapsid protein for cTAR DNA binding and destabilization, and correlation with inhibition of self-primed DNA synthesis. *J. Mol. Biol. 348*, 1113−1126.
(33) Narayanan, N., Gorelick, R. J., and DeStefano, J. J. (2006) Structure/function mapping of amino acids in the *N*-terminal zinc finger of the human immunodeficiency virus type 1 nucleocapsid protein: Residues responsible for nucleic acid helix destabilizing activity. *Biochemistry 45*, 12617−12628.
(34) Stoylov, S. P., Vuilleumier, C., Stoylova, E., De Rocquigny, H., Roques, B. P., Gérard, D., and Mély, Y. (1997) Ordered aggregation of ribonucleic acids by the human immunodeficiency virus type 1 nucleocapsid protein. *Biopolymers 41*, 301−312.
(35) Le Cam, E., Coulaud, D., Delain, E., Petitjean, P., Roques, B. P., Gérard, D., Stoylova, E., Vuilleumier, C., Stoylov, S. P., and Mély, Y. (1998) Properties and growth mechanism of the ordered aggregation of a model RNA by the HIV-1 nucleocapsid protein: an electron microscopy investigation. *Biopolymers 45*, 217−229.
(36) Krishnamoorthy, G., Roques, B., Darlix, J.-L., and Mély, Y. (2003) DNA condensation by the nucleocapsid protein of HIV-1: A mechanism ensuring DNA protection. *Nucleic Acids Res. 31*, 5425−5432.
(37) Mirambeau, G., Lyonnais, S., Coulaud, D., Hameau, L., Lafosse, S., Jeusset, J., Justome, A., Delain, E., Gorelick, R. J., and Le Cam, E. (2006) Transmission electron microscopy reveals an optimal HIV-1 nucleocapsid aggregation with single-stranded nucleic acids and the mature HIV-1 nucleocapsid protein. *J. Mol. Biol. 364*, 496−511.
(38) Vo, M.-N., Barany, G., Rouzina, I., and Musier-Forsyth, K. (2006) Mechanistic studies of mini-TAR RNA/DNA annealing in the absence and presence of HIV-1 nucleocapsid protein. *J. Mol. Biol. 363*, 244−261.
(39) de Rocquigny, H., Ficheux, D., Gabus, C., Fournié-Zaluski, M.-C., Darlix, J.-L., and Roques, B. P. (1991) First large scale chemical synthesis of the 72 amino acid HIV-1 nucleocapsid protein NCp7 in an active form. *Biochem. Biophys. Res. Commun. 180*, 1010−1018.
(40) Omichinski, J. G., Clore, G. M., Sakaguchi, K., Appella, E., and Gronenborn, A. M. (1991) Structural characterization of a 39-residue synthetic peptide containing the two zinc binding domains from the HIV-1 p7 nucleocapsid protein by CD and NMR spectroscopy. *FEBS Lett. 292*, 25−30.
(41) De Rocquigny, H., Gabus, C., Vincent, A., Fournié-Zaluski, M.-C., Roques, B., and Darlix, J.-L. (1992) Viral RNA annealing activities of human immunodeficiency virus type 1 nucleocapsid protein require only peptide domains outside the zinc fingers. *Proc. Natl. Acad. Sci. U.S.A. 89*, 6472−6476.
(42) Morellet, N., Jullian, N., De Rocquigny, H., Maigret, B., Darlix, J.-L., and Roques, B. P. (1992) Determination of the structure of the nucleocapsid protein NCp7 from the human immunodeficiency virus type 1 by ^{1}H NMR. *EMBO J. 11*, 3059−3065.
(43) Sakaguchi, K., Zambrano, N., Baldwin, E. T., Shapiro, B. A., Erickson, J. W., Omichinski, J. G., Clore, G. M., Gronenborn, A. M., and Appella, E. (1993) Identification of a binding site for the human immunodeficiency virus type 1 nucleocapsid protein. *Proc. Natl. Acad. Sci. U.S.A. 90*, 5219−5223.
(44) Surovoy, A., Dannull, J., Moelling, K., and Jung, G. (1993) Conformational and nucleic acid binding studies on the synthetic nucleocapsid protein of HIV-1. *J. Mol. Biol. 229*, 94−104.
(45) Dannull, J., Surovoy, A., Jung, G., and Moelling, K. (1994) Specific binding of HIV-1 nucleocapsid protein to PSI RNA *in vitro*

requires N-terminal zinc finger and flanking basic amino acid residues. *EMBO J. 13*, 1525−1533.
(46) Al-Ghusein, H., Ball, H., Igloi, G. L., Gbewonyo, A., Coates, A. R. M., Mascagni, P., and Roberts, M. M. (1996) Chemically synthesised human immunodeficiency virus P7 nucleocapsid protein can self-assemble into particles and binds to a specific site on the $tRNA^{Lys,3}$ primer. *Biochem. Biophys. Res. Commun. 224*, 191−198.
(47) Dong, C. Z., De Rocquigny, H., Rémy, E., Mellac, S., Fournié-Zaluski, M. C., and Roques, B. P. (1997) Synthesis and biological activities of fluorescent acridine-containing HIV-1 nucleocapsid proteins for investigation of nucleic acid-NCp7 interactions. *J. Pept. Res. 50*, 269−278.
(48) Hsu, M., Rong, L., de Rocquigny, H., Roques, B. P., and Wainberg, M. A. (2000) The effect of mutations in the HIV-1 nucleocapsid protein on strand transfer in cell-free reverse transcription reactions. *Nucleic Acids Res. 28*, 1724−1729.
(49) Takahashi, K., Baba, S., Koyanagi, Y., Yamamoto, N., Takaku, H., and Kawai, G. (2001) Two basic regions of NCp7 are sufficient for conformational conversion of HIV-1 dimerization initiation site from kissing-loop dimer to extended-duplex dimer. *J. Biol. Chem. 276*, 31274−31278.
(50) Baba, S., Takahashi, K., Koyanagi, Y., Yamamoto, N., Takaku, H., Gorelick, R. J., and Kawai, G. (2003) Role of the zinc fingers of HIV-1 nucleocapsid protein in maturation of genomic RNA. *J. Biochem. 134*, 637−639.
(51) Liu, H.-W., Cosa, G., Landes, C. F., Zeng, Y., Kovaleski, B. J., Mullen, D. G., Barany, G., Musier-Forsyth, K., and Barbara, P. F. (2005) Single-molecule FRET studies of important intermediates in the nucleocapsid-protein-chaperoned minus-strand transfer step in HIV-1 reverse transcription. *Biophys. J. 89*, 3470−3479.
(52) Riddles, P. W., Blakeley, R. L., and Zerner, B. (1983) Reassessment of Ellman's reagent. *Methods Enzymol. 91*, 49−60.
(53) Zuker, M. (2003) Mfold web server for nucleic acid folding and hybridization prediction. *Nucleic Acids Res. 31*, 3406−3415.
(54) Cruceanu, M., Urbaneja, M. A., Hixson, C. V., Johnson, D. G., Datta, S. A., Fivash, M. J., Stephen, A. G., Fisher, R. J., Gorelick, R. J., Casas-Finet, J. R., Rein, A., Rouzina, I., and Williams, M. C. (2006) Nucleic acid binding and chaperone properties of HIV-1 Gag and nucleocapsid proteins. *Nucleic Acids Res. 34*, 593−605.
(55) Gasteiger, E., Hoogland, C., Gattiker, A., Duvaud, S., Wilkins, M. R., Appel, R. D., and Bairoch, A. (2005) Protein Identication and Analysis Tools on the ExPASy Server. In *The Proteomics Protocols Handbook* (Walker, J. M., Ed.) pp 571−607, Humana Press, New York.
(56) Avilov, S. V., Piemont, E., Shvadchak, V., de Rocquigny, H., and Mély, Y. (2008) Probing dynamics of HIV-1 nucleocapsid protein/target hexanucleotide complexes by 2-aminopurine. *Nucleic Acids Res. 36*, 885−896.
(57) Bazzi, A., Zargarian, L., Chaminade, F., Boudier, C., De Rocquigny, H., René, B., Mély, Y., Fossé, P., and Mauffret, O. (2011) Structural insights into the cTAR DNA recognition by the HIV-1 nucleocapsid protein: Role of sugar deoxyriboses in the binding polarity of NC. *Nucleic Acids Res. 39*, 3903−3916.
(58) Mirambeau, G., Lyonnais, S., Coulaud, D., Hameau, L., Lafosse, S., Jeusset, J., Borde, I., Reboud-Ravaux, M., Restle, T., Gorelick, R. J., and Le Cam, E. (2007) HIV-1 protease and reverse transcriptase control the architecture of their nucleocapsid partner. *PLoS One 2*, e669.
(59) Mirambeau, G., Lyonnais, S., and Gorelick, R. J. (2010) Features, processing states, and heterologous protein interactions in the modulation of the retroviral nucleocapsid protein function. *RNA Biol. 7*, 724−734.
(60) Vo, M.-N., Barany, G., Rouzina, I., and Musier-Forsyth, K. (2009) Effect of Mg^{2+} and Na^{+} on the nucleic acid chaperone activity of HIV-1 nucleocapsid protein: Implications for reverse transcription. *J. Mol. Biol. 386*, 773−788.
(61) Anthony, R. M., and Destefano, J. J. (2007) *In vitro* synthesis of long DNA products in reactions with HIV-RT and nucleocapsid protein. *J. Mol. Biol. 365*, 310−324.
(62) DeRouchey, J., Hoover, B., and Rau, D. C. (2013) A comparison of DNA compaction by arginine and lysine peptides: A physical basis for arginine rich protamines. *Biochemistry 52*, 3000−3009.
(63) Wu, T., Heilman-Miller, S. L., and Levin, J. G. (2007) Effects of nucleic acid local structure and magnesium ions on minus-strand transfer mediated by the nucleic acid chaperone activity of HIV-1 nucleocapsid protein. *Nucleic Acids Res. 35*, 3974−3987.
(64) Sikorav, J. L., and Church, G. M. (1991) Complementary recognition in condensed DNA: Accelerated DNA renaturation. *J. Mol. Biol. 222*, 1085−1108.
(65) Christiansen, C., and Baldwin, R. L. (1977) Catalysis of DNA reassociation by the *Escherichia coli* DNA binding protein: A polyamine-dependent reaction. *J. Mol. Biol. 115*, 441−454.
(66) Miller Jenkins, L. M., Ott, D. E., Hayashi, R., Coren, L. V., Wang, D., Xu, Q., Schito, M. L., Inman, J. K., Appella, D. H., and Appella, E. (2010) Small-molecule inactivation of HIV-1 NCp7 by repetitive intracellular acyl transfer. *Nat. Chem. Biol. 6*, 887−889.
(67) Pannecouque, C., Szafarowicz, B., Volkova, N., Bakulev, V., Dehaen, W., Mély, Y., and Daelemans, D. (2010) Inhibition of HIV-1 replication by a bis-thiadiazolbenzene-1,2-diamine that chelates zinc ions from retroviral nucleocapsid zinc fingers. *Antimicrob. Agents Chemother. 54*, 1461−1468.
(68) Druillennec, S., Dong, C. Z., Escaich, S., Gresh, N., Bousseau, A., Roques, B. P., and Fournié-Zaluski, M. C. (1999) A mimic of HIV-1 nucleocapsid protein impairs reverse transcription and displays antiviral activity. *Proc. Natl. Acad. Sci. U.S.A. 96*, 4886−4891.
(69) Park, M. Y., Kwon, J., Lee, S., You, J., and Myung, H. (2004) Selection and characterization of peptides specifically binding to HIV-1 psi (ψ) RNA. *Virus Res. 106*, 77−81.
(70) Raja, C., Ferner, J., Dietrich, U., Avilov, S., Ficheux, D., Darlix, J.-L., de Rocquigny, H., Schwalbe, H., and Mély, Y. (2006) A tryptophan-rich hexapeptide inhibits nucleic acid destabilization chaperoned by the HIV-1 nucleocapsid protein. *Biochemistry 45*, 9254−9265.
(71) Dietz, J., Koch, J., Kaur, A., Raja, C., Stein, S., Grez, M., Pustowka, A., Mensch, S., Ferner, J., Möller, L., Bannert, N., Tampé, R., Divita, G., Mély, Y., Schwalbe, H., and Dietrich, U. (2008) Inhibition of HIV-1 by a peptide ligand of the genomic RNA packaging signal ψ. *ChemMedChem 3*, 749−755.
(72) Shvadchak, V., Sanglier, S., Rocle, S., Villa, P., Haiech, J., Hibert, M., Van Dorsselaer, A., Mély, Y., and de Rocquigny, H. (2009) Identification by high throughput screening of small compounds inhibiting the nucleic acid destabilization activity of the HIV-1 nucleocapsid protein. *Biochimie 91*, 916−923.
(73) Chung, J., Ulyanov, N. B., Guilbert, C., Mujeeb, A., and James, T. L. (2010) Binding characteristics of small molecules that mimic nucleocapsid protein-induced maturation of stem-loop 1 of HIV-1 RNA. *Biochemistry 49*, 6341−6351.
(74) Avilov, S. V., Boudier, C., Gottikh, M., Darlix, J.-L., and Mély, Y. (2012) Characterization of the inhibition mechanism of HIV-1 nucleocapsid protein chaperone activities by methylated oligoribonucleotides. *Antimicrob. Agents Chemother. 56*, 1010−1018.
(75) Breuer, S., Chang, M. W., Yuan, J., and Torbett, B. E. (2012) Identification of HIV-1 inhibitors targeting the nucleocapsid protein. *J. Med. Chem. 55*, 4968−4977.
(76) Mori, M., Schult-Dietrich, P., Szafarowicz, B., Humbert, N., Debaene, F., Sanglier-Cianferani, S., Dietrich, U., Mély, Y., and Botta, M. (2012) Use of virtual screening for discovering antiretroviral compounds interacting with the HIV-1 nucleocapsid protein. *Virus Res. 169*, 377−387.
(77) Quintal, S., Viegas, A., Erhardt, S., Cabrita, E. J., and Farrell, N. P. (2012) Platinated DNA affects zinc finger conformation. Interaction of a platinated single-stranded oligonucleotide and the C-terminal zinc finger of nucleocapsid protein HIVNCp7. *Biochemistry 51*, 1752−1761.
(78) Warui, D. M., and Baranger, A. M. (2012) Identification of small molecule inhibitors of the HIV-1 nucleocapsid-stem-loop 3 RNA complex. *J. Med. Chem. 55*, 4132−4141.
(79) Goudreau, N., Hucke, O., Faucher, A.-M., Grand-Maître, C., Lepage, O., Bonneau, P. R., Mason, S. W., and Titolo, S. (2013) Discovery and structural characterization of a new inhibitor series of

HIV-1 nucleocapsid function: NMR solution structure determination of a ternary complex involving a 2:1 inhibitor/NC stoichiometry. *J. Mol. Biol. 425*, 1982−1998.